Supplement of The Cryosphere, 19, 6001–6021, 2025 https://doi.org/10.5194/tc-19-6001-2025-supplement © Author(s) 2025. CC BY 4.0 License.





Supplement of

Seasonal evolution of snow density and its impact on thermal regime of sea ice during the MOSAiC expedition

Yubing Cheng et al.

Correspondence to: Bin Cheng (bin.cheng@fmi.fi)

The copyright of individual parts of the supplement might differ from the article licence.

Supplementary material

Seasonal evolution of snow density and its impact on thermal regime of sea ice during the MOSAiC expedition

Yubing Cheng¹, Bin Cheng², Roberta Pirazzini², Amy R. Macfarlane^{3,4}, Timo Vihma², Wolfgang Dorn¹, Ruzica Dadic⁵, Martin Schneebeli⁵, Stefanie Arndt⁶, and Annette Rinke¹

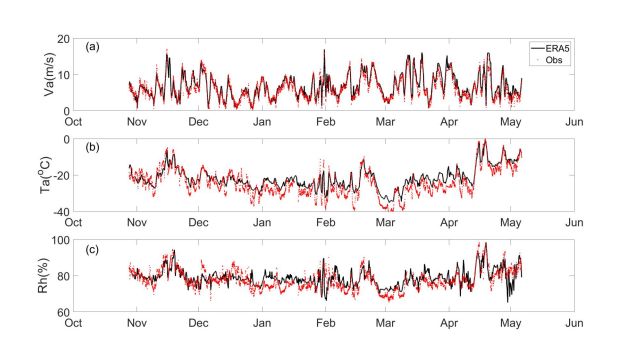
¹Alfred Wegener Institute, Helmholtz Centre for Polar and Marine Research, Potsdam, Germany

> ²Finnish Meteorological Institute, Helsinki, Finland ³The Arctic University of Norway UiT, Tromsø, Norway ⁴ Northumbria University, Newcastle Upon Tyne, UK

⁵ WSL Institute for Snow and Avalanche Research SLF, Davos Dorf, Switzerland
⁶Alfred Wegener Institute, Helmholtz Centre for Polar and Marine Research, Bremerhaven,

Germany

* Correspondences: bin.cheng@fmi.fi



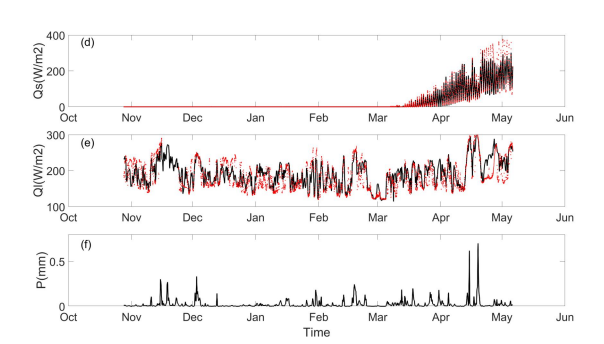


Figure S1. Time series of (a) wind speed (V_a) ; (b) air temperature (T_a) ; (c) relative humidity (Rh); (d) shortwave radiative flux (Q_s) ; (e) longwave radiative flux (Q_l) , and (f) snow precipitation rate (P). The red dots are in situ observations. The black lines are ERA5 reanalysis products extracted along the MOSAiC ice camp drift trajectory and used as weather forcing for HIGHTSI modelling. The observed Rh was calculated using the observed dew point temperature.

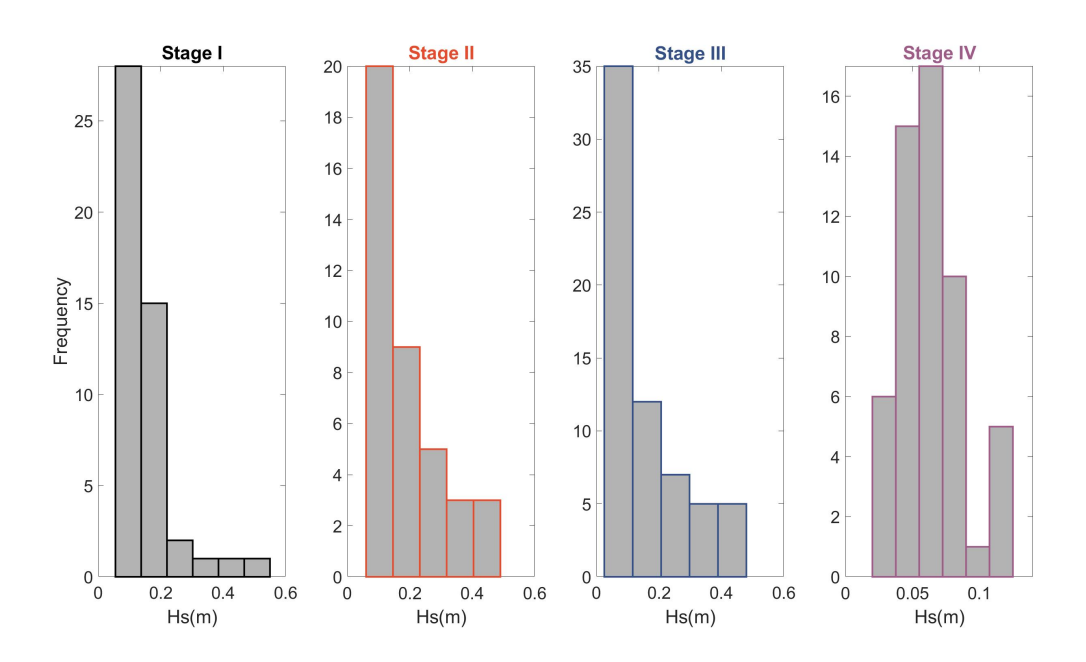


Figure S2. Frequency distribution of snow depth samples observed during each stage. In each stage, the number of samples is 49, 40, 64, and 56, respectively.

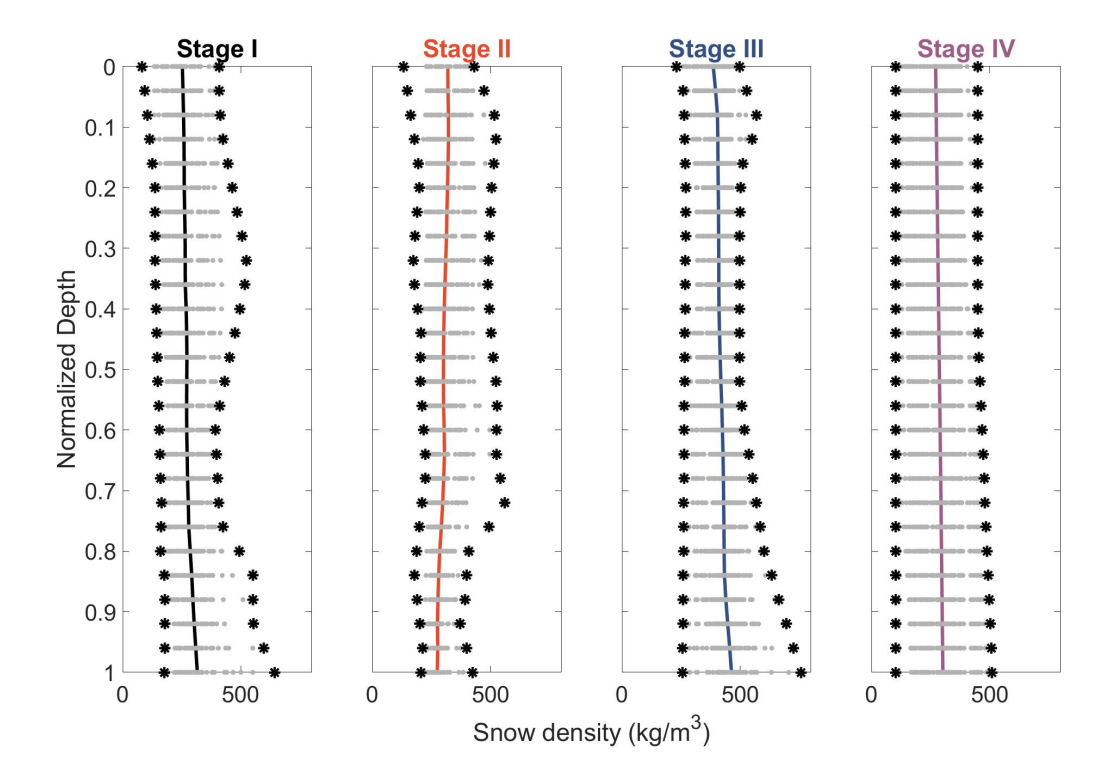


Figure S3. The spatial standard deviation of snow density across the sample sites (represented by horizontal bars) is shown at normalized interpolated vertical levels. The vertical lines represent the normalized mean snow density.

Table S1. Key weather, snow, and ice parameters for HIGHTSI model experiments.

Parameter	Value	Source	

$V_a, T_a, Rh, Q_s, Q_l, P$	Time series	ERA5	
Oceanic heat flux (F_w)	3 W m ⁻²	(Lei et al., 2022)	
Freezing point (T_f)	-1.8 °C	Literature	
Sea ice density (ρ_i)	910 kg m ⁻³	Literature	
Snow density* (ρ_0)	340 kg m ⁻³	(Wagner et al., 2022)	
Snow density (ρ_s)	Difference density schemes a	and observation time series	
Sea ice salinity (s_i)	4 ppt	(Angelopoulos et al 2022)	
Heat capacity of $ice(c_i)$	2093 J kg ⁻¹ K ⁻¹	Literature	
Latent heat of freezing (L_i)	$0.33 \times 10^6 \mathrm{Jkg^{-1}}$		
Initial ice thickness	0.36 m	MOSAiC Observations	
Initial snow depth	0.1 m		
Initial ice temperature	Linear interpolation between T_a and T_f		

^{*}This snow density is used to convert snow precipitation (expressed in SWE) to snow accumulation.

Table S2. Statistics of weather variables (hourly mean) during the modeling period (28 October 2019 – 6 May 2020) for ERA5 reanalysis products and ice camp observations (Obs).

Statistics		$V_a(\text{m/s})$	T _a (°C)	Rh (%)	$Q_s (W/m^2)$	$Q_l (W/m^2)$
Mean value	ERA5	6.7	-21.6	79	26	191
	Obs	6.2	-24.1	78	29	184
Standard deviation	ERA5	3.2	6.	4.5	59	36
	Obs	3.1	7.5	5.6	68	40
Maximum value	ERA5	17	-0.8	98	315	308
	Obs	17	-0.1	98	376	311
Minimum value	ERA5	0.6	-35	65	0.00	114
	Obs	0.3	-42	66	0.00	120
Bias		0.5	2.5	1.1	3	7
RMSE		1.2	4.0	4.0	19	26
Correlation coeff.		0.94	0.92	0.72	0.97	0.78

Data gap periods were excluded from comparisons.

References

Angelopoulos, M., Damm, E., Sim~oes Pereira, P., Abrahamsson, K., Bauch, D., Bowman, J., Castellani, G., Creamean, J., Divine, D.V., Dumitrascu, A., Fons, S.W., Granskog, M.A., Kolabutin, N., Krumpen, T., Marsay, C., Nicolaus, M., Oggier, M., Rinke, A., Sachs, T., Shimanchuk, E., Stefels, J., Stephens, M., Ulfsbo, A., Verdugo, J., Wang, L., Zhan, L.Y., Haas, C., 2022. Deciphering the properties of different Arctic ice types during the growth phase of MOSAiC: Implications for future studies on gas pathways. Front. Earth Sci. 10 https://doi.org/10.3389/feart.2022.864523.

Lei, R., Cheng, B., Hoppmann, M., Zhang, F., Zuo, G., Hutchings, J.K., Lin, L., Lan, M., Wang, H., Regnery, J., Krumpen, T., Haapala, J., Rabe, B., Perovich, D.K. and Nicolaus, M. 2021. Seasonality and timing of sea ice mass balance and heat fluxes in the Arctic transpolar drift during 2019–2020. Elem Sci Anth, 10: 1. DOI:

https://doi.org/10.1525/elementa.2021.000089

Wagner, D. N., Shupe, M. D., Cox, C., Persson, O. G., Uttal, T., Frey, M. M., Kirchgaessner, A., Schneebeli, M., Jaggi, M., Macfarlane, A. R., Itkin, P., Arndt, S., Hendricks, S., Krampe, D., Nicolaus, M., Ricker, R., Regnery, J., Kolabutin, N., Shimanshuck, E., Oggier, M., Raphael, I., Stroeve, J., and Lehning, M.: Snowfall and snow accumulation during the MOSAiC winter and spring seasons, The Cryosphere, 16, 2373–2402, https://doi.org/10.5194/tc-16-2373-2022, 2022.